RESEARCH ARTICLE

BON VIEW PUBLISHING

A Study of the Effects of the Shape Parameter and Type of Data Points Locations on the Accuracy of the Hermite-Based Symmetric Approach Using Positive Definite Radial Kernels

Stephen Mkegh Nengem[1],* and Friday Haruna[1]

[1]Taraba State University, Nigeria

Abstract: Theoretical approximation ideas served as the driving force behind the research. one can see that the shape parameter's behavior is driven by the kind of problem and the analytical standards that are applied. the primary issue here is not just how it impacts the interpolant's accuracy but also how quickly it converges, or how quickly the error reduces as the number of data nodes rises. Hence, this article considers two globally supported and positive radial kernels and three different patterns of data point locations on the same computational domain. The research specifically studied the effects of the shape parameter and the type of data points locations on the accurate performance of an Hermite-based symmetric approach. The two-dimensional Helmholtz equation and the two-dimensional Poisson equation were used as test functions. The problems were first solved on the three different types of data point locations using linear Laguerre-Gaussians and then, the linear Matern. In each case, the graph of the error against the shape parameter was drawn to enable easy identification of the optimal value of the shape parameter. One important result indicated that, an improved accuracy cannot be achieved without the appropriate value of the shape parameter irrespective of the type of data site used.

Keywords: radial kernel, shape parameter, positive definite, uniformly spaced data points, scattered data points, Chebyshev's data points

1. Introduction

Our research is motivated from the theoretical principles of approximation. Basically, the behavior of the shape parameter is dependent on the type of problem (de Marchi & Perracchione, 2018). It also depends on the criteria how one is able to analyze it. The main problem here is not just how it affects the accuracy of the interpolant, but also its convergence rate, the rate at which the error decreases as the number of data nodes increases. It can be found in literatures by some researchers such Fasshauer and McCourt (2015), and Fasshauer (2007) that, to get the optimal convergence in terms of the global kernels on smooth target functions, small shape parameters are necessary, because the smooth shape parameters give more global basis. This assertion gives us a better enablement for recovering the spectral convergence. Depending on the issue one have at hand, much larger values of the shape parameter often result in unphysical behavior that leads to ill-conditioning (Fasshauer & McCourt, 2015).

There is a number of modern algorithm that has recently spring up in attempt to absolutely get rid of the ill-conditioning stemming from parameterization. One of the current bests is the Radial Basis Function-Genetic Algorithm RBF-GA algorithm, though limited to Gaussian RBFs (Hosseini, 2018). This was a variant on the RBF-QR

technique that Fornberg and Piret (2008) proposed. Other recent approaches such as the Hilbert–Schmidt Singular Value Decomposition SVD approach that was developed by Fasshauer and McCourt (2015) can be compared to be equivalent to the RBF-QR. However, these approach the problem from the sense of Mercer's theorem, which is based on eigen-function evaluations. de Marchi and Santin (2015) studied an approach refers to as weighted SVD method, which combines well with any radial kernel and their shape parameters but again need a quadrature/cubature rule, and that only settled the issue of the ill-conditioning partly. Some other interesting algorithms such as the Contour–Pade algorithm, which considers the radial kernel interpolating function as a monomorphic function, use contour integration technique to overcome the pole singularity problem (Yensiri & Skulkhu, 2017). And its recent variant, the RBF-RA approach, almost substitutes the Pade approximation techniques in the Contour–Pade method with a rational approximant (Ghalichi et al., 2022).

According to Wendland (2005), smaller shape parameter limit is very important when considering the connections of radial kernels to interpolation functions, Fourier series, and spherical harmonics. Considering one dimension on Chebyshev's nodes, as the shape parameter ε approaches zero, you are sure to reproduce the polynomial interpolant. On the other hand, on a circle, as the shape parameter approaches zero, the spherical RBFs recover the Fourier interpolant. On a sphere, they reproduce the spherical harmonics. In two dimensional

*Corresponding author: Stephen Mkegh Nengem, Taraba State University, Nigeria. Email: nengem.stephen@tsuniversity.edu.ng

spaces and higher, if the nodal set is polynomial unisolvent, the radial kernel interpolant will recover that polynomial in this limit (Zhao, 2016).

From the literature considered so far, it is carefully noticed that the success of reproducing a function from a set of data also depends on the type of the structure of the data sampling; poor data structure/sampling may lead to a poor recovery form (Zhao, 2016). It was also observed that the type of kernel used and the shape parameter play a very important role for optimal recovery (Krowiak & Podgórski, 2017). In view of this, it is of great interest that the problem of finding, characterizing, and/or constructing optimal shape parameter values and data structures to maximize accuracy be given due to attention. The particular kernels and how to identify their optimal shape parameters to be used for the interpolation and approximation problem become prominent.

Thus, in the light of the advantages of the globally supported radial bases methods, in particular Hermite-based symmetric approach for recovery of functions from scattered data. We studied the effects of the shape parameter and the type data locations on the accuracy of this approach using positive definite radial kernels for the solution of partial differential equations. Since radial kernels are the category of functions that have the free parameter called the shape parameter which requires attention for their effective implementation. Their choices have a tremendous impact on the accuracy of the results and the numerical global stability of the method used. We showed in this work that an Hermite-based approach which is one of the radial kernels' methods requires a careful choice of the shape parameter value with a unique type of data point location for a better accuracy. We also showed that each problem may have its own optimal shape parameter and the type of data point location.

This numerical scheme has so many applications ranging across problems that involve determining the unknown values that lie in between the known data points. It is most times used to predict the unknown values for any geographical related data points such as noise, rainfall, and elevation. This also has applications in image reproduction.

2. An Hermite-Based Approach for Differential Operators

Let us contemplate on the set of scattered data nodes $x_i \in \mathbb{R}^d$, $i = 1, \ldots, N^I$. Assuming that at each of these data nodes, a function value $f(x_i) = f_i$ is given. More also, at some of these data nodes x_j^D, $j = N^I + 1, \ldots, N$ we have known values of the function's derivatives given at those points denoted by $(D_j f)(x_j) = Df_j$, where D_j is a differential operator which act on the function at j^{th} node (de Marchi & Santin, 2015; Liu & Li, 2018). We supposed here that there should be only one derivative value at each one data node, although one can easily extend the problem to more than one derivative.

Now, we want to estimate an approximate value for the function at any other point different from the given nodes. According to Nengem (2023), to analyze the function by tools made available in mathematical analysis, an interpolation series involving radial kernels is recommended in the following form:

$$\tilde{u}(x) = \sum_{j=1}^{N^I} \alpha_j \varphi(\mathcal{E}\|x - c\|)\big|_{c=x_j^I} + \sum_{j=N^I+1}^{N} \alpha_j \left[D_j^c \varphi(\mathcal{E}\|x - c\|) \right]_{c=x_j^D} \tag{1}$$

where $\varphi(\mathcal{E}\|x - c\|)$ represents the radial kernel function, whose values depend on the distance from an interpolation point x to a fixed point c, called the center. In practice, the centers often coincide with the data nodes x_i. In Equation (1) α_j, β_j are interpolation coefficients and

D_j^c denote the differential operator which is acting on the function at x_j^d node. In the understanding, the function was looked upon as the function of c variable (Krowiak & Podgórski, 2017; Scholkopf & Smola, 2002). In order to find the suitable interpolation coefficients, the following interpolation conditions are enforced on the function as follows:

$$\sum_{j=1}^{N^I} \alpha_j \varphi(\mathcal{E}\|x_i - c\|)\big|_{c=x_j}$$

$$+ \sum_{j=N^I+1}^{N} \beta_j \left[D_j^c \varphi(\mathcal{E}\|x_i - c\|) \right]_{c=x_j^D} = f_i, \quad i = 1, \ldots, N^I \tag{2}$$

as well as for its derivatives:

$$\sum_{j=1}^{N^I} \alpha_j \left[D_j^x \varphi(\mathcal{E}\|x - c\|) \right]_{\substack{c = x_j \\ x = x_i^D}}$$

$$+ \sum_{j=N^I+1}^{N} \beta_j \left[D_j^x \left[D_j^c \varphi(\mathcal{E}\|x - c\|) \right]_{c=x_j^D} \right]_{x=x_i^D} = Df_i \tag{3}$$

$$i = N^I + 1, \ldots, N$$

In Equation (3), D_j^x refer to the same differential operator as D^c but now acting on the radial kernel as a function of the x variable. This makes the coefficient matrix of the Equations (2) and (3) a symmetric one, which make its assembling and solution of the problem easier (Chen et al., 2022). This system can be rewritten in a more convenient and simplified way using the matrix notation:

$$\begin{bmatrix} A & A_{D^c} \\ A_{D^x} & A_{D^x D^c} \end{bmatrix} \cdot \begin{bmatrix} \alpha \\ \beta \end{bmatrix} = \begin{bmatrix} f \\ Df \end{bmatrix} \tag{4}$$

where

$$A_{i,j} = \varphi(\mathcal{E}\|x_i - c\|)\big|_{c=x_j}, \quad i, j = 1, \ldots, N^I$$

$$(A_{D^c})_{i,j} = [D^c \varphi(\mathcal{E}\|x_i - c\|)]_{c=x_j^D}, \quad i = 1, \ldots, N^I, \quad j = N^I + 1, \ldots, N$$

$$(A_{D^x})_{i,j} = [D^x \varphi(\mathcal{E}\|x - c\|)]_{\substack{c = x_j, \\ x = x_i^D}}$$

$$i = N^I + 1, \ldots, N, \quad j = 1, \ldots, N^I$$

$$(A_{D^x D^c})_{i,j} = \left[D^x [D^c \varphi(\mathcal{E}\|x - c\|)]_{c=x_j^D} \right]_{x=x_i^D},$$

$$i = N^I + 1, \ldots, N, \quad j = N^I + 1, \ldots, N$$

α, β and f, Df are the interpolation coefficients, function values, and their derivatives, respectively. In order to find the values of the interpolation coefficients, the Equation (4) has to be solved yielding

$$\begin{bmatrix} \alpha \\ \beta \end{bmatrix} = \begin{bmatrix} A & A_{D^c} \\ A_{D^x} & A_{D^x D^c} \end{bmatrix}^{-1} \cdot \begin{bmatrix} f \\ Df \end{bmatrix}$$

The solvability of the system depends on the type of the kernel used. In many cases, the Equation (1) has to be augmented by a polynomial term to guarantee the invertibility of the system matrix (Fornberg, 2021; Speckbacher & Balazs, 2020). In this work, we shall use

two radial kernels: the linear Laguerre–Gaussian and the Matern function, which are globally supported and positive definite to investigate their suitability in Hermite-based interpolation approach and in the solution of elliptic partial differential equation with a pretty focused on the role of their shape parameter.

3. The Shape Parameter

Consider a given data set, $X = \{x_j\}_{j=1}^N$, containing N distinct interpolation points, suppose we have an unknown function u, collated at the same given points in the domain Ω. Any radial kernel interpolant $\tilde{u}$, containing a shape parameter ε, can be written as (Karageorghis & Tryfonos, 2019)

$$\tilde{u}(x_j, \varepsilon) = u(x_j), \quad \text{for each } j = 1, \ldots, N. \qquad (5)$$

Then, we see that there exists a lower bound which limits the maximum error of each given radial kernel interpolation presented as

$$\max_{x \in \Omega}\{|\tilde{u}(x, \varepsilon) - u(x)|\} \geq \max_{x_j \in X}\{|\tilde{u}(x_j, \varepsilon) - u(x_j)|\} \qquad (6)$$

In other words, the accuracy of a given radial kernel interpolant is always optimal at the sampled points. Considering the shape parameter ε, it can be choosing in such a way as to improve the accuracy of the numerical result. According to Kuo (2015), if an optimal solution of radial kernel interpolation exists in terms of shape parameter ε, then the ideal ε value should be located at

$$\max_{x \in \Omega}\{|\tilde{u}(x, \varepsilon) - u(x)|\} \approx \max_{x_j \in X}\{|\tilde{u}(x_j, \varepsilon) - u(x_j)|\} \qquad (7)$$

The simplest strategy to find the optimal shape parameter is to perform a series of interpolation experiments with varying shape parameter and then to select the best one which minimizes the error (Beezer, 2015). This strategy can be the best practice if we know the function u that produces the data, and thus, it can calculate some sort of error for the interpolant. Definitely, if we already know u, then the job of looking for the interpolant may be needless. However, that is the strategy use in the academic. But if we do not have any singular knowledge of the function u, then it is extremely difficult to say what optimal means. One criterion to do this is based on the trade-off principle, that is, based on the fact that for small values of ε, the error improves while the condition number grows. The optimal value is then defined to be the smallest ε for which MATLAB did not issue a near-singular warning (Aggarwal et al., 2021).

In many instances, selection of an optimal shape parameter via trial by error will end up being a rather tedious process. However, this is presently the method or approach that is used by most researchers (Karageorghis & Tryfonos, 2019). Since all values of the shape parameter contributes to the accuracy of the approximation, Ghalichi et al. (2022) proposed an algorithm for choosing a good shape parameter value by minimizing a cost function which imitates the error between the radial kernel interpolant and the unknown function.

In this work, we use the brute force method to compute a suitable estimate for the shape parameter ε. The brute force method consists of performing various interpolation experiments with different values of the shape parameter ε. The best value of the shape parameter is the one that minimizes the interpolation error, both root mean square and maximum error (Esmaeilbeigi et al., 2018). This is achieved by plotting the interpolation error against the shape parameter. The minimum point on the curve gives the optimal value of the shape parameter ε. We shall plot both RMS-error and max-error

against different values of the shape parameter and select the value at the minimum point to be an estimate use for the experiment. The experiments will be carried out on the computational domain $\Omega = [0, 1] \times [0, 1]$ with three different patterns of data point locations, namely uniformly spaced data points, scattered data points (Halton sequence), and the Chebyshev's data points to check the most suitable. The radial kernels used in this set of experiments are the linear Matern and the linear Laguerre Gaussian.

The radial kernels used and their derivatives up to second order of the data are given below. The choice of radial kernels to use for the experiment was arbitrary.

Linear Laguerre–Gaussians

$$\varphi(r) = e^{-(\varepsilon r)^2}(2 - (\varepsilon r)^2), \text{ where } r = \|x\| = \sqrt{x^2 + y^2}$$

$$\frac{\partial}{\partial x}\varphi(r) = 2\varepsilon^2 x e^{-(\varepsilon r)^2}((\varepsilon r)^2 - 3),$$

$$\frac{\partial}{\partial y}\varphi(r) = 2\varepsilon^2 y e^{-(\varepsilon r)^2}((\varepsilon r)^2 - 3)$$

$$\frac{\partial^2}{\partial x^2}\varphi(r) = -2\varepsilon^2 e^{-(\varepsilon r)^2}(2(\varepsilon x)^2((\varepsilon r)^2 - 4) - (\varepsilon r)^2 + 3),$$

$$\frac{\partial^2}{\partial y^2}\varphi(r) = -2\varepsilon^2 e^{-(\varepsilon r)^2}(2(\varepsilon y)^2((\varepsilon r)^2 - 4) - (\varepsilon r)^2 + 3),$$

$$\frac{\partial^2}{\partial xy}\varphi(r) = -4\varepsilon^4 xy e^{-(\varepsilon r)^2}((\varepsilon r)^2 - 4),$$

Linear Matern

$$\varphi(r) = e^{-(\varepsilon r)}((\varepsilon r) + 1), \text{ where } r = \|x\| = \sqrt{x^2 + y^2}$$

$$\frac{\partial}{\partial x}\varphi(r) = -\varepsilon^2 x e^{-(\varepsilon r)},$$

$$\frac{\partial}{\partial y}\varphi(r) = -\varepsilon^2 y e^{-(\varepsilon r)},$$

$$\frac{\partial^2}{\partial x^2}\varphi(r) = \varepsilon^2 e^{-(\varepsilon r)}\left(\frac{\varepsilon x^2}{r} - 1\right),$$

$$\frac{\partial^2}{\partial y^2}\varphi(r) = \varepsilon^2 e^{-(\varepsilon r)}\left(\frac{\varepsilon y^2}{r} - 1\right),$$

$$\frac{\partial^2}{\partial xy}\varphi(r) = \varepsilon^3 xy e^{-(\varepsilon r)^2}/r.$$

4. Numerical Studies

The investigation is carried out using the two-dimensional Helmholtz equation as a test function taken from Thounthong et al. (2018).

$$u_{xx} + u_{yy} + ku(x, y) = f(x, y), \quad (x, y) \in [0, 1]^2 \qquad (8)$$

with $k = -5$, and the function $f(x, y)$ is specified, so that the exact solution is

$$u(x, y) = e^{xy}(x^2 - x)^2(y^2 - y)^2 \qquad (9)$$

And the two-dimensional Poisson equation (Cavoretto & de Rossi, 2010) is

$$\nabla^2 u + x u_x + y u_y - (4x^2 + y^2)u = f(x, y), \qquad (10)$$

$$(x, y) \in [a, b]^2$$

where $f(x, y)$ and the Dirichlet boundary conditions are computed from the exact solution, which is given by:

$$u(x, y) = \exp(x^2 + 0.5y^2) \qquad (11)$$

The results are obtained using the Hermite-based symmetric approach. The radial kernels used for this implementation are the linear Matern and the linear Laguerre–Gaussians with the optimal shape parameter chosen from the set of experiments using brute force method. The root mean square error and maximum error are calculated for the corresponding values of ε. Results are reported in the Tables and Figures and below for $N = 81$. The results are presented for uniformly spaced, scattered and Chebyshev data points. Max-error is the maximum absolute squared deviation of the data set from the approximation solution, and the RMS-error is the root mean squared norm of the difference between the data and the approximation divided by the number of elements.

5. Discussion

Figure 1 shows the pictorial representation of the three different types of data points locations used for the experiment. Figure 1(a) is the uniformly spaced data sites, Figure 1(b) is the randomly scattered data site, and Figure 1(c) is the Chebyshev's type of data site. Tables 1 and 2 show results of the interpolation errors at two different shape parameter values with the least errors using linear Laguerre–Gaussians and linear Matern, respectively. The linear Laguerre–Gaussians gave the most accurate result on uniformly spaced data points at the shape parameter value $\varepsilon = 2$ as seen in Table 1, while the linear Matern produced the best accuracy on scattered data points at the shape parameter value $\varepsilon = 4$ as seen in Table 2. Although linear Laguerre–Gaussians produced the overall best accurate result for test problem 1, and that was achieved using the uniformly spaced data points, we can see that the linear Laguerre–Gaussians falls short in terms of accuracy on scattered data points. Figures 2 and 3 show the errors of the interpolation against the shape parameter using linear Laguerre–Gaussians and linear Matern, respectively, for problem 1, and Figures 4 and 5 show the errors of the interpolation against the shape parameter using linear Laguerre–Gaussians and linear Matern, respectively, for problem 2. The red line corresponds to the root-mean-square error, and the blue line represents the maximum error. In Figure 2, the optimal shape parameter is $\varepsilon = 2$ using uniformly spaced and Chebyshev's data points and $\varepsilon = 7.5$ using scattered data points. In Figure 2, the optimal shape parameter is $\varepsilon = 2$ using uniformly spaced and Chebyshev's data points and $\varepsilon = 7.5$ using scattered data points, while, in Figure 3, the optimal shape parameter occurred at different points: $\varepsilon = 4$ using uniformly spaced data points, $\varepsilon = 6.7$ using scattered data points, and $\varepsilon = 7$ Chebyshev's data point. We found here that varying shape parameter did produce a better interpolation than using a constant shape parameter.

Similarly, Tables 3 and 4 show results of the interpolation errors at two different shape parameter values with the least errors using linear Laguerre–Gaussians and linear Matern, respectively, using three data structures. The linear Laguerre–Gaussians produced the most accurate result on uniformly spaced data points at the shape parameter value $\varepsilon = 0.5$ as seen in Table 3, while the linear Matern performed almost the same on uniformly spaced and Chebyshev's

Figure 1
Types of data points locations used: (a) equally spaced data points, (b) scattered data points, and (c) the Chebyshev's data points
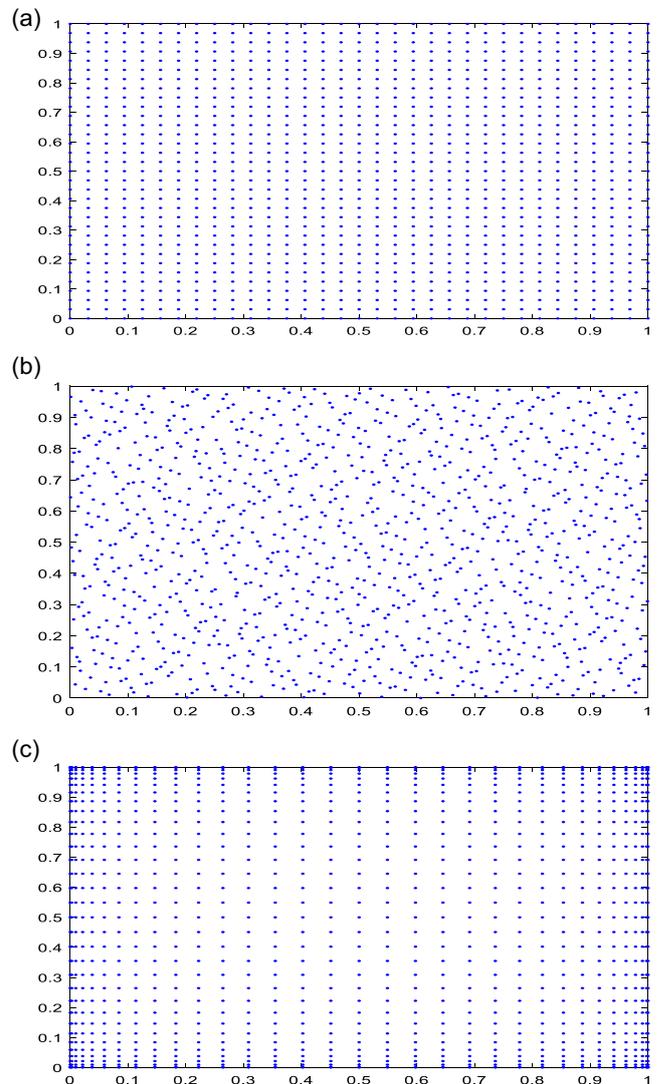

Table 1
Numerical results for example problem 1 using linear Laguerre–Gaussians on the three types of data points

Mesh	RBF	ε	RMS_Error	Max_Error
Solution on a domain containing equally spaced data points				
81	LL Gaussians	2	6.297425×10^{-6}	2.787099×10^{-5}
81	LL Gaussians	5	3.378711×10^{-5}	1.038160×10^{-4}
Solution on a domain containing scattered data points				
81	LL Gaussians	2	1.433326×10^{-4}	1.977825×10^{-3}
81	LL Gaussians	5	7.082516×10^{-5}	5.031587×10^{-4}
Solution on a domain containing Chebyshev's type of data points				
81	LL Gaussians	2	8.514199×10^{-6}	4.201340×10^{-5}
81	LL Gaussians	4.5	7.275635×10^{-5}	2.617018×10^{-4}

Figure 2
Errors for example problem with 81 (a) uniformly spaced, (b) randomly distributed, and (c) Chebyshev's data points using linear Laguerre–Gaussians

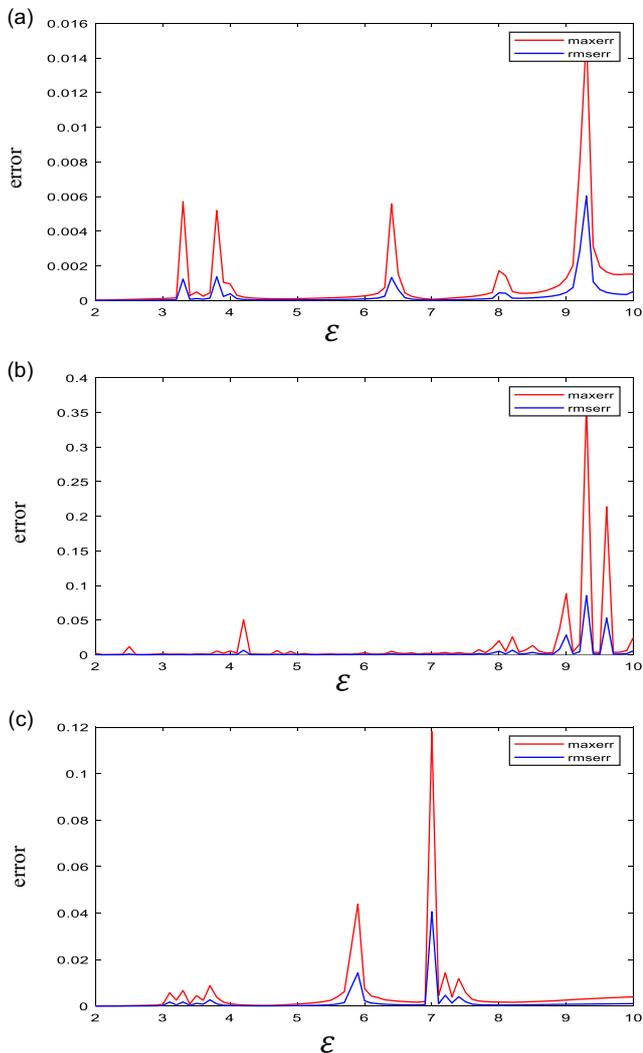
Figure 3
Errors for example problem 1 with 81 (a) uniformly spaced (b) randomly distributed and (c) Chebyshev's data points using linear Matern
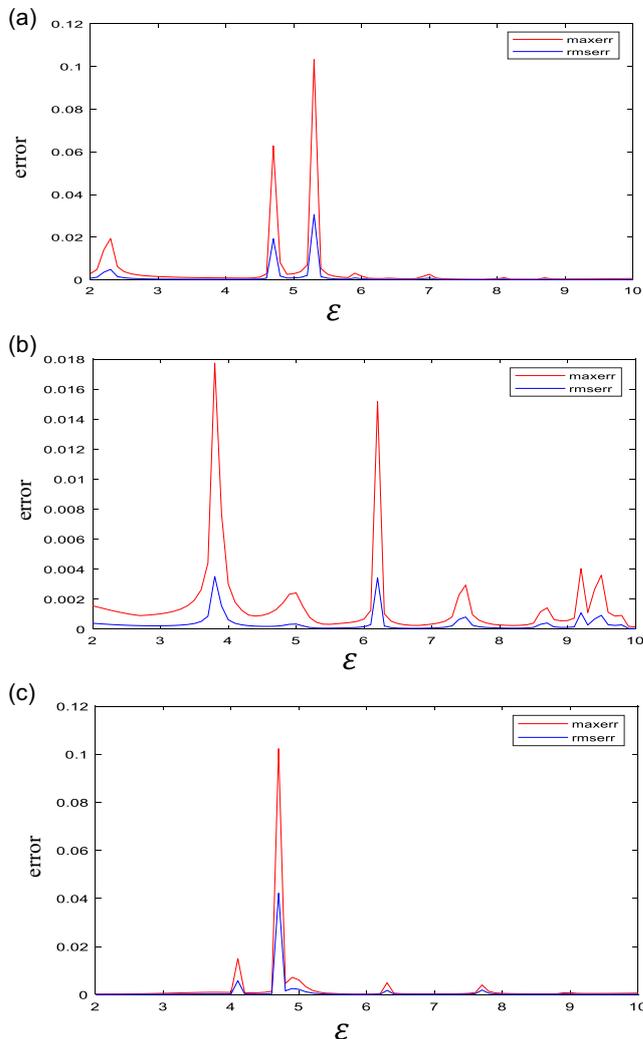

Table 2
Numerical results for example problem 1 using linear Matern on the three types of data points

Mesh	RBF	ε	RMS_Error	Max_Error
Solution on a domain containing equally spaced data points				
81	L Matern	4	9.967807×10^{-5}	3.071871×10^{-4}
81	L Matern	7	1.801439×10^{-4}	6.230061×10^{-4}
Solution on a domain containing scattered data points				
81	L Matern	4	7.406272×10^{-5}	4.106071×10^{-4}
81	L Matern	6.7	9.337209×10^{-5}	3.444061×10^{-4}
Solution on a domain containing Chebyshev's type of data points				
81	L Matern	4	1.662238×10^{-4}	5.040811×10^{-4}
81	L Matern	7	1.355145×10^{-4}	4.751625×10^{-4}

Table 3
Numerical results for example problem 2 using linear Laguerre–Gaussians on the three types of data points

Mesh	RBF	ε	RMS_Error	Max_Error
Solution on a domain containing equally spaced data points				
81	LL Gaussians	0.5	9.972636×10^{-8}	4.296176×10^{-8}
81	LL Gaussians	1	1.764559×10^{-8}	2.543928×10^{-7}
Solution on a domain containing scattered data points				
81	LL Gaussians	1	1.443721×10^{-7}	1.957225×10^{-6}
81	LL Gaussians	2	4.152576×10^{-8}	2.133547×10^{-7}
Solution on a domain containing Chebyshev's type of data points				
81	LL Gaussians	0.5	7.312112×10^{-8}	5.281310×10^{-8}
81	LL Gaussians	1	3.125605×10^{-8}	1.013018×10^{-6}

Figure 4
Errors for example problem with 81 (a) uniformly spaced, (b) randomly distributed, and (c) Chebyshev's data points using linear Laguerre–Gaussians
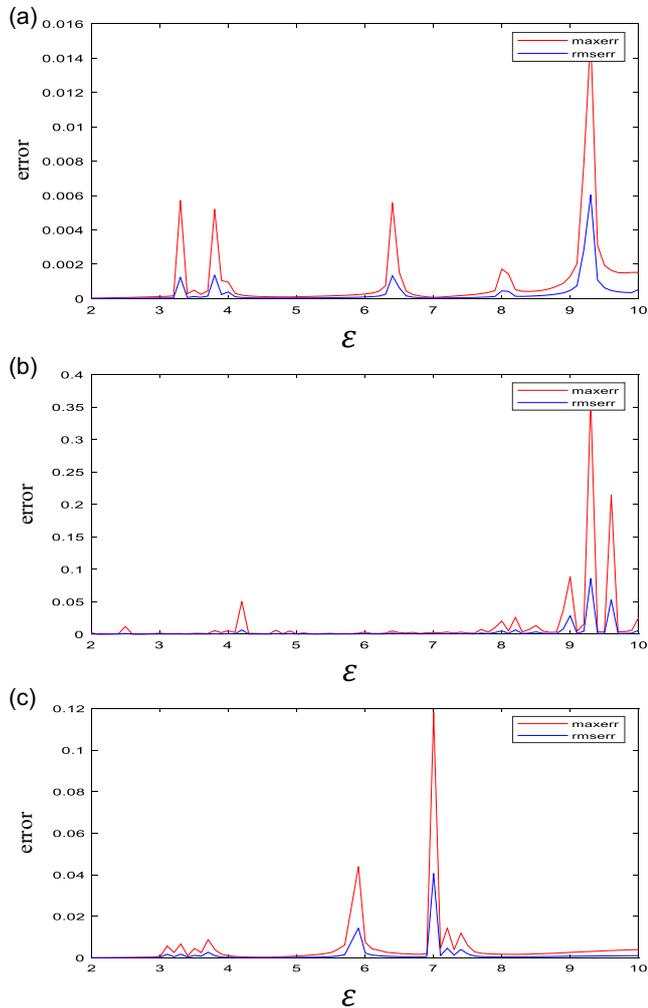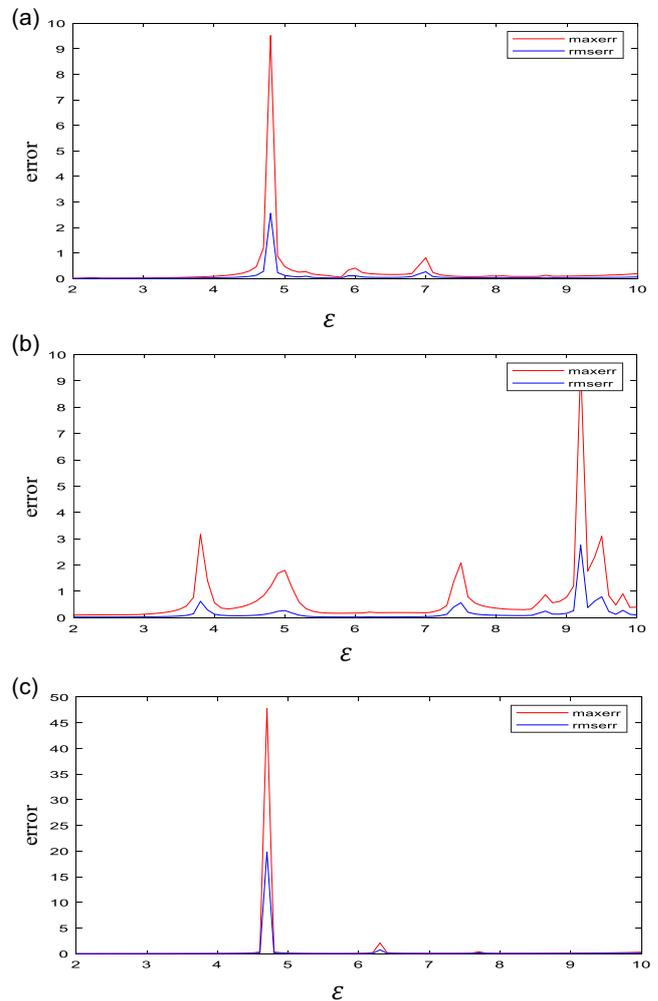

Figure 5
Errors for example problem with 81 (a) uniformly spaced, (b) randomly distributed, and (c) Chebyshev's data points using linear Matern

data points at the shape parameter value $\varepsilon = 0.5$ and 1, respectively, as seen in Table 4. The linear Laguerre–Gaussians produced the overall best accurate result for test problem 2, and that was achieved

Table 4
Numerical results for example problem 2 using linear Matern on the three types of data points

Mesh	RBF	ε	RMS_Error	Max_Error
Solution on a domain containing equally spaced data points				
81	L Matern	0.5	1.465020×10^{-7}	4.484514×10^{-7}
81	L Matern	1	3.077793×10^{-7}	1.745657×10^{-6}
Solution on a domain containing scattered data points				
81	L Matern	2	3.221943×10^{-7}	1.441125×10^{-6}
81	L Matern	4	9.095941×10^{-7}	5.959408×10^{-6}
Solution on a domain containing Chebyshev's type of data points				
81	L Matern	1	1.282886×10^{-7}	9.896830×10^{-7}
81	L Matern	4	1.108630×10^{-6}	6.647000×10^{-6}

using the uniformly spaced data points. In Figures 4 and 5, the optimal shape parameter is $\varepsilon = 0.5$ using uniformly spaced and Chebyshev's data points and $\varepsilon = 1$ using scattered data points. We also found here that varying shape parameter did produce a better interpolation than using a constant shape parameter.

There were no clear determining factors on where and/or at what shape parameter value will the best interpolation occur for a particular test problem, but one is likely to get the optimal value of ε around the origin, since the errors seems to converged for the values of ε around the origin.

6. Conclusions

It is concluded that an improved accuracy cannot be achieved without the appropriate value of the shape parameter irrespective of the type of data site used. It is also concluded that the type of data points location used is also very important to achieving the best result even at the optimal shape parameter value. Thus, to achieve the best result, the shape parameter and the unique type of data point locations to use for the particular problem should be given due to attention.

Some of the challenges encountered in the process of implementation were how to find the optimal shape parameter and ill-conditioning of the interpolation matrix. The optimal shape parameter though was achieved by drawing the graph of the shape parameter against error. The value with the minimal error was chosen as the optimal value. The ill-conditioning problem was checked using GMRES, a preconditioning technique for a better and improved accuracy.

Acknowledgments

Conflicts of Interest

The authors declare that they have no conflicts of interest to this work.

Data Availability Statement

Data available on request from the corresponding author upon reasonable request.

References

Aggarwal, R., Lamichhane, B. P., Meylan, M. H., & Wensrich, C. M. (2021). An investigation of radial basis function method for strain reconstruction by energy-resolved neutron imaging. *Applied Sciences*, *11*(1), 391.

Beezer, R. A. (2015). *A first course in linear algebra*. USA: Congruent Press.

Cavoretto, R., & de Rossi, A. (2010). Fast and accurate interpolation of large scattered data sets on the sphere. *Journal of Computational Applied Mathematics*, *234*(5), 1505–1521. https://doi.org/10.1016/j.cam.2010.02.031

Chen, Y. T., Li, C., Yao, L. Q., & Cao, Y. (2022). A hybrid RBF collocation method and its application in the elastostatic symmetric problems. *Symmetry, 14*(7), 1476. https://doi.org/10.3390/sym14071476

de Marchi, S., & Perracchione, E. (2018). *Lectures on radial basis functions*. Italy: University of Padua.

de Marchi, S., & Santin, G. (2015). Fast computation of orthonormal basis for RBF spaces through Krylov space methods. *BIT Numerical Mathematics*, *55,* 949–966. https://doi.org/10.1007/s10543-014-0537-6

Esmaeilbeigi, M., Chatrabgoun, O., & Shafa, M. (2018). Scattered data fitting of Hermite type by a weighted meshless method. *Advances in Computational Mathematics*, *44*, 673–691. https://doi.org/10.1007/s10444-017-9555-7

Fasshauer, G. E., & McCourt, M. J. (2015). *Kernel-based approximation methods using Matlab*. Singapore: World Scientific Publishing Company.

Fasshauer, G. E. (2007). *Meshfree approximation methods with MATLAB*. Singapore: World Scientific Publishing Co. Pte. Ltd, 520pp.

Fornberg, B. (2021). An algorithm for calculating Hermite-based finite difference weights. *IMA Journal of Numerical Analysis*, *41*(2), 801–813. https://doi.org/10.1093/imanum/draa006

Fornberg, B., & Piret, C. (2008). A stable algorithm for flat radial basis functions on a sphere. *SIAM Journal on Scientific Computing*, *30*(1), 60–80. https://doi.org/10.1137/060671991

Ghalichi, S. S. S., Amirfakhrian, M., & Allahviranloo, T. (2022). An algorithm for choosing a good shape parameter for radial basis functions method with a case study in image processing. *Results in Applied Mathematics*, *16*, 100337. https://doi.org/10.1016/j.rinam.2022.100337

Hosseini, S. (2018). Numerical solution of the first-order evolution equations by radial basis function. *International Journal of Mathematical Modelling & Computations*, *8*(1), 61–66.

Karageorghis, A., & Tryfonos, P. (2019). Shape parameter estimation in RBF function approximation. *International Journal of Computational Methods and Experimental Measurements*, *7*(3), 246–259.

Krowiak, A., & Podgórski, J. (2017). Hermite interpolation of multivariable function given at scattered points. *Technical Transactions*, *8*, 199–205. https://doi.org/10.4467/2353737XCT.17.142.6893

Kuo, L. H. (2015). *On the selection of a good shape parameter for RBF approximation and its application for solving PDEs*. PhD Thesis, The University of Southern Mississippi.

Liu, J., & Li, X. (2018). A novel Hermite RBF-based differential quadrature method for solving two-dimensional variable-order time fractional advection-diffusion equation with Neumann boundary condition. *arXiv Preprint:1809.02301*. https://doi.org/10.48550/arXiv.1809.02301

Nengem, S. M. (2023). Symmetric kernel-based approach for elliptic partial differential equation. *Journal of Data Science and Intelligence Systems, 1*(2), 99–104. https://doi.org/10.47852/bonviewJDSIS3202884

Scholkopf, B., & Smola, A. (2002). *Learning with kernels: Support vector machines, regularization, optimization, and beyond*. USA: MIT Press.

Speckbacher, M., & Balazs, P. (2020). Frames, their relatives and reproducing kernel Hilbert spaces. *Journal of Physics A: Mathematical and Theoretical*, *53*(1), 015204. https://doi.org/10.1088/1751-8121/ab573c

Thounthong, P., Khan, M. N., Hussain, I., Ahmad, I., & Kumam, P. (2018). Symmetric radial basis function method for simulation of elliptic partial differential equations. *Mathematics*, *6*(12), 327. https://doi.org/10.3390/math6120327

Wendland, H. (2005). *Scattered data approximation*. UK: Cambridge University Press.

Yensiri, S., & Skulkhu, R. J. (2017). An investigation of radial basis function-finite difference (RBF-FD) method for numerical solution of elliptic partial differential equations. *Mathematics*, *5*(4), 54. https://doi.org/10.3390/math5040054

Zhao, Y. (2016). *Multilevel sparse grid kernels collocation with radial basis functions for elliptic and parabolic problems*. PhD Thesis, University of Leicester.